Published in final edited form as:
Bioconjug Chem. 2012 December 19; 23(12): 2451–2459. doi:10.1021/bc300549s.

Synthesis and Characterization of a Melanoma-Targeted Fluorescence Imaging Probe by Conjugation of a Melanocortin 1 Receptor (MC1R) Specific Ligand

Narges K Tafreshi[†], **Xuan Huang**[†], **Valerie E Moberg**[†], **Natalie M. Barkey**[†], **Vernon K. Sondak**[‡], **Haibin Tian**[†], **David L Morse**[†,*], and **Josef Vagner**[§,*]

[†]Dept. Cancer Imaging and Metabolism, H. Lee Moffitt Cancer Center & Research Institute, Tampa, FL

[‡]Department of Cutaneous Oncology, H. Lee Moffitt Cancer Center & Research Institute, Tampa, FL

[§]BIO5 Institute, University of Arizona, Tucson, AZ

Abstract

The incidence of malignant melanoma is rising faster than that of any other cancer in the United States. The melanocortin 1 receptor (MC1R) is overexpressed in most human melanoma metastases, thus making it a promising target for imaging and therapy of melanomas. We have previously reported the development of a peptidomimetic ligand with high specificity and affinity for MC1R. Here, we have conjugated near-infrared fluorescent dyes to the C-terminus of this ligand via lysine-mercaptopropionic acid linkers to generate MC1R specific optical probes (MC1RL-800, 0.4 nM K_i and MC1RL-Cy5, 0.3 nM Ki). Internalization of the imaging probe was studied *in vitro* by fluorescence microscopy using engineered A375/MC1R cells and B16F10 cells with endogenous MC1R expression. The *in vivo* tumor targeting of MC1RL-800 was evaluated by intravenous injection of probe into nude mice bearing bilateral subcutaneous A375 xenograft tumors with low MC1R expression and engineered A375/MC1R tumors with high receptor expression. Melanotic B16F10 xenofgrafts were also studied. Fluorescence imaging showed that the agent has higher uptake values in tumors with high expression compared to low ($p<0.05$), demonstrating the effect of expression levels on image contrast-to-noise. In addition, tumor uptake was significantly blocked by co-injection of excess NDP-α-MSH peptide ($p<0.05$). In conclusion, the MC1R-specific imaging probe developed in this study displays excellent potential for the intraoperative detection of regional node involvement and for margin detection during melanoma metastasis resection.

INTRODUCTION

Malignant melanoma is the most lethal form of skin cancer and one of the fastest increasing cancers in the US.[1, 2] About 16% of patients develop metastases over time.[3, 4] The most common metastatic sites are regional lymph nodes, lung, liver, and brain.[5] Surgery remains the mainstay of melanoma therapy at all sites, if it is technically feasible and risk of

[*]Corresponding Authors: J. V., The BIO5 Institute, University of Arizona, 1657 E Helen Street, Tucson, Arizona 85721, Phone 520-626-4179, fax 520-626-4824; vagner@email.arizona.edu; and D.L.M., H. Lee Moffitt Cancer Center and Research Institute, 12902 Magnolia Drive, Tampa, FL 33612; David.Morse@moffitt.org.

Supporting Information Available: This information is available free of charge via the Internet at http://pubs.acs.org/

Disclosure of Potential Conflicts of Interest: No potential conflicts of interest were disclosed.

morbidity and mortality is low and the patient is likely to live long enough to accrue benefit.[5, 6]

The complete removal of tumor during surgery is dependent on the surgeon's ability to differentiate tumor from normal tissue using subjective criteria that are not easily quantifiable. A real-time visualization of cancer cells with high-resolution during surgery in patients would be of great value and there is great interest in approaches that can optimize surgical margins at the initial surgery.[7, 8]

Currently, ultrasound and x-ray fluoroscopy are the two imaging techniques that are most utilized during human surgery. However, ultrasound requires direct contact with tissue and only sees a thin "slice" of the surgical field-of-view. When x-ray fluoroscopy is used, the patient and caregivers are exposed to ionizing radiation. Importantly, neither of these methods are tumor-specific, since targeted contrast agents are not available (reviewed in [9]). In contrast, near-infrared real-time fluorescence imaging (700-900 nm), as an optical technique, offers the possibility of actively imaging the resection cavity in real-time as the surgery progresses, providing superior resolution and sensitivity [8], high tissue penetration up to several millimeters deep, and low autofluorescence, providing a favorable signal-to-noise ratio. In addition, several near-infrared fluorescent (NIRF) dyes are available for chemical conjugation to molecules that can target tumors, e.g. antibodies or peptides (reviewed by [10]).

Intraoperative sentinel lymph node biopsy (SLNB) is widely used for staging of melanoma, and the pathologic status of the sentinel lymph node is reported to be one of the most important prognostic indicators.[11, 12] However, SLNB is associated with morbidity.[13, 14] SLNB typically involves the use of blue dye and/or radiocolloid to detect the sentinel nodes followed by removal and histologic examination to determine pathologic status. The radiocolloid and dyes currently used for SLNB are not tumor specific and, hence, cannot directly detect lymph node involvement. Indocyanine green (ICG) NIRF dye has been used intraoperatively for SLNB [15], although it is not tumor specific. Therefore, NIRF-labeled melanoma targeted imaging agents would allow the intraoperative detection of regional metastasis in lymph nodes, directing the biopsy of only lymph nodes with suspected involvement, and potentially decreasing SLNB associated morbidities.

The amount of the surrounding normal skin that needs to be excised around a primary cutaneous melanoma has been a controversial issue among surgeons [6] and development of melanoma targeted imaging probes for intraoperative evaluation of margin status of melanoma lesions as well as melanoma metastasis resection has potential to improve the outcome of the surgery. Such a probe would also allow for intraoperative detection of regional lymph nodes bearing metastases. In addition, there is increasing interest in the use of novel targeted therapies for treatment of malignant melanomas that are resistant to most systemic therapies.[16]

Melanoma progression is associated with altered expression of cell surface proteins, including adhesion proteins and receptors.[17-19] It has been estimated that over 80% of malignant melanomas express high levels of the MC1R [20], making it one of the very few specific targets potentially useful for diagnosis and therapy of metastatic melanoma.[21-23] MC1R is a member of a family of five G protein-coupled receptors (MC1R – MC5R) for melanocortins.[24-26] Melanocortin receptors are expressed in a wide range of tissues and organs throughout the body, ranging from the hair and skin (MC1R), kidneys and lungs (MC5R), adrenal glands (MC2R), and hypothalamus (MC3R/MC4R) (see [27] for review). Peptide ligands have been developed, e.g. [Nle^4,D-Phe^7]-α-MSH (NDP-α-MSH), that have high binding affinities for MC1R, MC3R, MC4R and MC5R, and these ligands have been investigated extensively.[28-31] However, these ligands are not selective for MC1R and such

off-target binding is undesirable given the presence of these receptors in clearance organs such as the kidney.

To discover a ligand with high affinity and specificity for MC1R, we have previously screened eight ligands against cell lines engineered to overexpress MC1R, MC4R or MC5R.[32] MC3R was excluded from these analyses as these peptide ligands are not expected to cross the blood-brain barrier. One of the compounds (4-phenylbutyryl-His-DPhe-Arg-Trp-Gly-Lys) exhibited high (0.2 nM) binding affinity for MC1R and low (high nanomolar) affinities for MC4R and MC5R. In the current study, by conjugating a near-infrared fluorescent dye (IRDye800CW from Li-Cor) as well as Cy5 to this ligand, we have developed MC1R-specific molecular imaging probes and characterized their tumor cell specificity, binding and uptake *in vitro*. In addition, the probe was used to image MC1R expression *in vivo* following intravenous injection into nude mice bearing bilateral high- and low-MC1R expressing xenograft tumors.

The NIRF molecular imaging probe developed in this study has potential for real-time intraoperative detection of regional melanoma lymph node metastases and margin detection of melanoma metastasis to lung, liver, brain and other sites during surgery.

EXPERIMENTAL PROCEDURE

Cell culture

A375 human malignant melanoma cells and melanotic B16F10-Luc mouse melanoma cells were grown in Dulbecco's Modified Eagle's Medium (DMEM) containing 10% fetal bovine serum, 100 units/mL penicillin and 100 μg/mL streptomycin in 5% CO_2 at 37°C. The A375 and B16F10-Luc were obtained from American Type Culture Collection (ATCC) and Caliper Life Sciences respectively, expanded for two passages and cryopreserved. All experiments were performed with cells of passage number less than 25 for A375 cells and 50 for B16F10-Luc cells. Cells were authenticated as negative for mycoplasma by testing at the ATCC and were monitored by microscopy and confirmed to maintain morphological traits over subsequent passages.

Generation of stably transfected A375 cells bearing the MC1R gene

Vector pCMV6 containing *homo sapiens* MC1R and neomycin as a selection marker was purchased (Origene). To identify the optimal concentration for selection, a range (100-1000 μg/ml) of G418 was tested on cells. A375 cells were transfected with 5 μg of the vector. In response to G418, massive cell death was observed after ~5 days. After 2 weeks, resistant colonies appeared. Large colonies were selected and transferred to individual plates. The clone with the highest expression of *MC1R* was determined using qRT-PCR as previously described.[33] *MC1R* specific primer sets were designed using Gene Runner Software for Windows version 3.05: forward, 5′-AATGTCATTGACGTGATCACCTG-3′ and reverse, 5′-GCAGTGCGTAGAAGATGGAGAT-3′. β-actin was used for normalization.[33] A clone with the highest expression was selected and maintained in medium containing 300 μg/ml of G418.

Characterization of hMC1R expression on A375 cells by immunocytochemistry (ICC)

To verify the cell surface expression of hMC1R, two sets of A375 (parental) and A375/hMC1R cells were plated at a cell density of 1×10^4 cells/well on glass coverslips placed at the bottom of culture wells and incubated for 16 hours. Cells were then treated with 30 μg/ml MC1R antibody (Almone Labs) and 5.0 μg/mL of WGA (Invitrogen) at 4°C for 10 minutes, washed 3 times with PBS, fixed with cold methanol:acetone (1:1) and air dried for 20 minutes. Plates were washed 3 times with warm PBS and incubated with 1:2000

secondary antibody (Alexa-Fluor 680 goat anti-mouse IgG, Invitrogen). After three washes with PBS, coverslips were mounted with mounting medium and DAPI. Samples were viewed in the Moffitt Analytical Microscopy Core Facility using an automated Zeiss Observer Z.1 inverted microscope using 40×/1.3NA oil immersion objectives through narrow bandpass DAPI and FITC /A488 Chroma filter cubes and Nomarski Differential Interference Contrast polarizing and analyzing prisms. Images were produced using the AxioCam MRm CCD camera and Axiovision version 4.6 software suite (Carl Zeiss Inc., Germany). Image Pro Plus 6.2 software (Mediacybernetics Inc.) was used to measure the probe-related fluorescence intensity per image.

Probe synthesis, purification and characterization

Materials—N^{α}-Fmoc protected amino acids, HBTU, and HOBt were purchased from SynPep (Dublin, CA) or from Novabiochem (San Diego, CA). Rink amide Tentagel S resin was acquired from Rapp Polymere (Tubingen, Germany). The following side chain protecting groups were used for the amino acids: Arg(N^{g}-Pbf); His(N^{im}-Trt); Trp(N^{in}-Trt); and Lys(N^{e}-Aloc).

IRDye800CW maleimide dye was purchased from Li-Cor (Lincoln, NE). Cy5 maleimide dye was purchased from Li-Cor (Lincoln, NE). Peptide synthesis solvents, dry solvents, and solvents for HPLC (reagent grade), and 4-phenylbutyric acid, were acquired from VWR (West Chester, PA) or Sigma-Aldrich, and were used without further purification unless otherwise noted. Compounds were manually assembled using 5 to 50 mL plastic syringe reactors equipped with a frit and Domino manual synthesizer obtained from Torviq (Niles, MI). The C-18 Sep-Pak™ Vac RC cartridges for solid phase extraction were purchased from Waters (Milford, MA).

Peptide Synthesis—Ligands were synthesized on Tentagel Rink amide resin (initial loading: 0.2 mmol/g) using N^{α}-Fmoc protecting groups and a standard DIC/HOBt or HBTU/HOBt activation strategy. The resin was swollen in THF for an hour, washed with DMF, and Fmoc protecting group removed with 20% piperidine in DMF (2 min + 20 min). The resin was washed with DMF, DCM, 0.2 M HOBt in DMF and finally with DMF, and the first amino acid coupled using pre-activated 0.3 M HOBt ester in DMF (3 eq. of N^{α}-Fmoc amino acid, 3 eq. of HOBt and 6 eq. of DIC). An on-resin test using Bromophenol Blue was used for qualitative and continuous monitoring of reaction progress. To avoid deletion sequences and slower coupling rate in longer sequences, the double coupling was performed at all steps with 3 eq. of amino acid, 3 eq. of HBTU and 6 eq. of DIEA in DMF. Any unreacted NH_2 groups on the resin thereafter were capped using an excess of 50% acetic anhydride in pyridine for 5 min. When the coupling reaction was finished, the resin was washed with DMF, and the same procedure was repeated for the next amino acid until all residues were coupled.

Aloc Cleavage—The orthogonal protecting Aloc group of C-terminal Lys was cleaved as follows. The resin was washed with DCM then flushed with argon for 10 min. A cleavage mixture of dimethylbarbituric acid (5 equiv.), $Pd(TPP)_4$ (0.2 equiv.) in DCM (0.5 M solution) was flushed with argon and injected into the syringe. The reaction mixture was stirred for 30 min then repeated. The resin was washed with DMF, 10% DIEA in DMF, DMF, 2% sodium diethyldithiocarbamate trihydride, 10% DIEA in DMF, DCM and DMF. The Trt-Mpr was attached to the free amine via HBTU coupling as described above.

Cleavage of ligand from the resin—A cleavage cocktail (10 mL per 1 g of resin) of TFA (91%), water (3%), triisopropylsilane (3%), and 1,2-ethylenedithiol (3%) was injected into the resin and stirred for 4 h at room temperature. The crude ligand was isolated from the

resin by filtration, the filtrate was reduced to low volume by evaporation using a stream of nitrogen, and the ligand was precipitated in ice-cold diethyl ether, washed several times with ether, dried, dissolved in water and lyophilized to give off-white solid powders that were stored at −20°C until purified. The crude compound was purified by size-exclusion chromatography.

Labeling procedure—The purified thiol compound (1 μmol) was dissolved in 1 mL DMF and reacted with 1 equiv. of IRDye800CW or Cy5 maleimide under argon atmosphere. The reaction was monitored by HPLC and additional aliquots (0.1 equiv.) of dye were added until completion of the reaction. The compound was purified by HPLC.

Purification and analysis—Purity of the peptides was ensured using analytical HPLC (Waters Alliance 2695 separation model with a dual wavelength detector Waters 2487) with a reverse-phase column (Waters Symmetry, 3.0 75 mm, 3.5 μm; flow rate = 0.3 mL/min) (Conditions: HPLC, linear gradient from 10 to 90% B over 30 min, where A is 0.1% TFA and B is acetonitrile). The HPLC traces for compounds are shown in Supplementary data as proof of purity (Figure S1 and S2). Size exclusion chromatography was performed on a borosilicate glass column (2.6 × 250 mm) filled with medium sized Sephadex G-25 or G-10. The compounds were eluted with an isocratic flow of 1.0 M aqueous acetic acid. Solid-Phase Extraction (SPE) was employed where simple isolation of final compound was needed from excess salts and buffers. For this purpose, C-18 Sep-Pak™ cartridges (100 mg or 500 mg) were used and pre-conditioned initially with 5 column volumes (5 times the volume of packed column bed) each of acetonitrile, methanol, and water, in that order. After loading the compound, the column was washed several times with water, and then gradually with 5, 10, 20, 30, 50 and 70% of aqueous acetonitrile to elute the peptide. Structures were characterized by ESI (Finnigan, Thermoquest LCQ ion trap instrument), MALDI-TOF or FT-ICR mass spectrometry. An appropriate mixture of standard peptides was used for internal calibrations. For compound MC1RL-800, MS calculated and measured (M+2)/2 was 1127.7 and 1127.9, respectively and for MC1RL-Cy5, MS calculated and measured (M +2)/2 was 921.9 and 922.0, respectively.

Binding assays

A375 melanoma cells engineered to express MC1R were used to assess ligand binding in a competitive binding assay as described before [32].

The receptor number of A375/MC1R (engineered cells to express MC1R) was determined using saturation binding assay following a previously described method [34], except that Eu-DTPA labeled NDP-α-MSH was used as a test ligand and 5 μM of NDP-α–MSH was used as a blocking ligand. These cells were used as a MC1R high expressing line, while the parental (A375) cells were used as a low expressing line with 400 ± 93 MC1R/cell.[35]

In vitro MC1R probe uptake study

To study the uptake of the MC1R probe *in vitro*, A375 (parental), A375/hMC1R (engineered cells for MC1R expression) and B16F10 cells (melanotic MC1R endogenous expressing cells) were plated at a cell density of 1×10^4 cells/well on glass coverslips placed at the bottom of culture wells and incubated for 16 hours. Cells were incubated in media containing 15 nM probe and uptake evaluated by fluorescence microscopy at different time points from 40 seconds to 15 minutes. To determine specificity, MC1R receptors were blocked by a 10 minute pre-incubation with 2 μM of NDP-α-MSH prior to addition of MC1R probe and images acquired 1 minute after addition of labeled probe. Samples were viewed using an Axio Observer Z1 inverted fluorescence microscope (Carl Zeiss, Inc, Germany) using 40×/1.3NA oil immersion objectives through a narrow band Cy5 filter. Cy5

fluorescence images were prepared with a DIC overlay image using Axiovision 4.6 software (Carl Zeiss, Inc, Germany).

Log D

The log of the octanol-water partition coefficient at pH 7.4 (log $D_{7.4}$) was determined by miniaturized shake flask assay. Briefly, (200μL to 1mL) n-octanol (Sigma) was added to a solution of the test compound prepared in PBS (25 mM NaH_2PO_4/Na_2HPO_4 buffer, pH 7.4, Sigma, HPLC grade). Then, three different ratios of octanol to PBS buffer were prepared. The mixture was stirred in a vortex mixer at room temperature for 1 min and then two layers were separated by centrifuge. The concentration of compound in each layer was determined by HPLC (Poroshell 120 EC-C18 column) using (26% acetonitrile in water, 0.1% TFA) in 280 nm channel. All sample injections were performed 3 times, and the results were averaged to yield the final values.

Tumor xenograft studies and fluorescence imaging

Male *nu/nu* mice 6-8 weeks old (Harlan Sprague Dawley, Inc., Indianapolis, IN) were injected subcutaneously (s.c.) with 1×10^6 MC1R expressing A375 cells in the right flank and the same number of parental cells in the left flank. Tumor volume was determined with calipers using the formula: volume = (length × width^2)/2. Once tumors reached 500-800 mm^3, 3 nmol/kg of either MC1RL-800 or MC1RL-Cy5 in 100 μL sterile saline was injected into the tail vein. *In vivo* fluorescence images were acquired using the Optix-MX3 (Advanced Research Technologies, Inc. a subsidiary of SoftScan Healthcare Group, Montreal, Canada). For the blocking study, 3 nmol/kg of probe was co-injected with 0.25 μg of the melanocortin receptor-specific ligand, NDP-α-MSH (Sigma) and animals were imaged similarly. Animals were positioned on a heating pad and anesthetized using isoflurane (flow 2–2.5 l/min). Fluorescence images were acquired using a scan resolution of 1.5 mm and a 790-nm pulsed laser diode with 40 MHz frequency and 12 ns time window. Images were analyzed using Optix-MX3 Optiview Software (version 3.01). Autofluorescence background was subtracted by determining the mean tumor fluorescence signal prior to injection, then mean normalized intensity values were obtained within a ROI on these images.

For B16F10 xenografts, 1×10^6 cells were injected s.c. into the right flank and allowed to grow to a volume of 500-800 mm^3, 3 nmol/kg of MC1R targeted imaging probe was injected into the tail vein and mice were then imaged using the Optix MX3 and FMT 2500 LX quantitative fluorescence tomography *in vivo* imaging system (PerkinElmer), which acquires both 2D surface fluorescence reflectance images (FRI) as well as 3D fluorescence molecular tomographic (FMT) imaging datasets. Using image data from phantoms containing known concentrations of the imaging probe and TrueQuant software v3.0 (PerkinElmer), the *in vivo* fluorescence data were quantitatively reconstructed to provide three-dimensional fluorescence tomography images and probe concentrations within the tumors.

MC1R IHC staining of xenograft tumors was performed in the Moffitt Tissue Core facility. Tumors were excised and fixed in formalin and embedded in paraffin for histology and fine sectioning. Formalin-fixed sections (5 μm) were IHC stained with rabbit MC1R polyclonal antibody (GTX70735, GeneTex), 1:200 dilution. The slides were scanned in the Moffitt Analytical Microscopy Core Facility using a ScanScope XT digital slide scanner (Aperio, CA). Positivity (number of positive pixels/total pixels number) of each slide was determined using Positive Pixel Count v9 Aperio Toolbox® software.

Statistics

Data are represented as mean ± s.d.. All statistical analyses were performed with GraphPad Prism version 5.01. Unpaired Student's t-test was used to determine the statistical significance of differences between two independent groups of variables. For all tests, a $p \leq 0.05$ was considered significant.

RESULTS AND DISCUSSION

Characterization of MC1R expression in A375/MC1R cells

A375 malignant melanoma cells were transfected to stably overexpress MC1R for evaluation of the MC1R imaging probes both *in vitro* and *in vivo*. The A375 malignant melanoma cell line was chosen due to its very low endogenous expression of MC1R[35, 36], providing both low- and high-expressing cells for the *in vitro* as well as *in vivo* selectivity studies. qRT-PCR of A375 and A375/MC1R cells revealed the level of MC1R mRNA expression to be ~100 fold higher in the engineered cells compared to the parental cell line. For further confirmation, hMC1R expression on the cell surface of the cells was characterized through ICC (Figure 1). Both engineered A375/hMC1R and parental A375 cells were incubated with the nuclear marker DAPI, the plasma membrane marker WGA and an MC1R antibody conjugated to a fluorescent dye (Alexa 555). The merged images illustrate co-localization of MC1R (red) with membrane marker (WGA, green) indicating accumulation of the receptor on the cell-surface (yellow). Notably, the parental A375 line does appear to have a detectable amount of MC1R antibody binding to the cell surface and the MC1R-related (red) fluorescence intensity was 8.5 fold higher in the engineered A375/MC1R cells compared to the A375 cells.

To determine MC1R receptor number on the cell surface, saturation binding assays were performed using Eu-NDP-α-MSH. Increasing amounts of Eu-NDP-α-MSH were added to A375/MC1R cells. Binding specificity was determined in the presence of melanocortin-receptor specific blocking ligand, 5 μM unlabeled NDP-α-MSH (Figure 2A). Results indicate that the Kd, Bmax and receptor number were 1.8 nM, 668,046 ± 67,108 and 75,000 respectively.

Synthesis and characterization of MC1R targeted probes

It has been known that MC1R ligands also show cross-reactivity with other melanocortin receptors. Since MC5R is expressed in kidney and lung, MC1R ligands with off-target binding to MC5R are not ideal for targeting of melanoma in patients. Recently our group described a high affinity peptidomimetic ligand against MC1R. K_i values for this ligand against MC1R, MC4R and MC5R were 0.24 nM, 254 nM and 46 nM, correspondingly, demonstrating very low interaction against MC4R and MC5R, 1000 and 200 times lower affinity compared with MC1R, respectively.[32] The use of small peptidomimetics as carriers for the delivery of imaging or therapeutic moieties to diseased tissues offers several advantages such as high biostability, ease of synthesis and modification, faster blood clearance, high-affinity and high-specificity, and low toxicity and immunogenicity. [37-41]

Here, we describe the attachment of a NIRF dye IRDye800CW as well as Cy5 to the C-terminus of the MC1R specific ligand via lysine-mercaptopropionic acid linker (4-phenylbutyryl-His-DPhe-Arg-Trp-Gly-Lys(Mpr-IRDye800CW)-NH_2, LiCor IRDye800CW Maleimide) to generate MC1RL-800 and MC1RL-Cy5 (Scheme 1). The sequence of this ligand was reported previously to have a high affinity and selectivity for MC1R [22, 42] and it was consequently chosen as a template for the design of the novel ligands.[32]

To evaluate the binding affinity of the MC1RL-800 and MC1RL-Cy5 probes, competition binding assays were preformed on A375/hMC1R cells with Eu-NDP-α-MSH as the competed ligand (Figure 2B). The MC1RL-800 and MC1R-Cy5 probes retained high affinity for MC1R, with a K_i of 0.4 ± 0.1 nM and 0.3 ± 0.05 nM , respectively, which is comparable to the K_i for the unlabeled ligand of 0.24 nM Ki.[32]

Cellular and tumor uptake studies

To study uptake of the MC1R probe by cells, MC1RL-Cy5 was incubated with live cells and images were acquired at different time-points after incubation using an inverted fluorescence microscope. Binding of probe to the surface of A375/MC1R cells was observed as early as 15 seconds after incubation and intracellular accumulation was observed within 5 minutes (Figure 3A). Therefore, the ligand could also be used in the clinic as a MC1R targeted delivery vehicle for radionuclides, toxins, and chemotherapeutic molecules. No binding or uptake of probe was observed when 2 μM NDP-α-MSH was used as a blocking agent before adding the probe to the cells (Figure 3A). Probe uptake was also observed (Figure 3B) by melanotic B16F10 cells that endogenously express MC1R (~22,000 ± 4200 MC1R/cell [35]) and blocking of probe-uptake was also observed in these cells. The blocking studies demonstrate the specificity of the probes for melanocortin receptor.

Determination of log D of MC1RL-800

To measure lipophilicity of the probe, log D (distribution co-efficient) was determined. Lipophilicity is a key determinant of the pharmacokinetic behavior of drugs and can influence distribution into tissues, absorption and the binding characteristics of a drug, as well as determination of the solubility of a compound (reviewed by [43]). The log D of MC1RL-800 probe was calculated to be −3.10 ± 0.13, suggesting that the probe is highly soluble in aqueous buffer and that the probe would have low permeability across the gastrointestinal tract or blood brain barrier.

In vivo tumor targeting

To investigate tumor targeting of the probe *in vivo*, bilateral subcutaneous xenograft tumors were established with A375/MC1R engineered cells in the right flank, and A375 parental cells with relatively low MC1R expression in the left flank. After tumor growth to approximately 500-800 mm^3, MC1RL-800 or MC1RL-Cy5 probe was injected intravenously and fluorescence accumulation was monitored over time. For both probes, the A375 tumors with low MC1R expression had significantly lower normalized fluorescence signal compared to A375/MC1R tumors 4 h post-injection ($P \leq 0.05$, n=3) (Figure 4A and 4B). *In vivo* blocking studies were performed to determine that probe retention in the tumor was due to specific binding. MC1RL-800 probe (3 nmol/kg) was co-injected with 0.25 μg of the melanocortin receptor-specific ligand, NDP-α-MSH. After blocking, the probe-related fluorescence signal decreased 1.7 fold in the A375/MC1R tumors ($p \leq 0.02$, n=3) and 1.4 fold in A375 tumors ($p \leq 0.05$, n=3) relative to the unblocked tumor at 4 h after injection (Figure 4A).

MC1R expression ranges from several hundred to around 10,000 receptors per cell in different human cell lines.[20] Therefore, development of a non-invasive imaging method for visualizing and quantifying MC1R expression will be useful for monitoring alterations in MC1R expression as an indicator of treatment response.[44] Our *in vivo* results indicate that the MC1RL-800 imaging probe related fluorescence was 2.0 ± 0.4 fold higher in the high expressing tumor relative to the low expressing tumor. This increase is lower than expected based on the receptor number per cell as determined *in vitro* in cultured cells by saturation binding assay, i.e the level of MC1R expression in A375 melanoma cells is 400 ± 93 sites/cell [35] compared to 75,000 sites/cell in the A375/MC1R cells which is a 190 fold difference.

However by comparing the same cell lines using ICC fluorescence, MC1R expression was determined to be only 8.5 fold higher. Also, proteins expression in cultured cell lines are known to differ from that of tumor xenografts using the same cell line. Such discrepancies are common throughout literature and undoubtedly play a role in the increased sensitivity of cancer cell lines to chemotherapy relative to solid tumors [45]. IHC staining of A375/MC1R xenograft tumors for MC1R was 2.0 ± 0.2 fold higher compared A375 tumors, which is nearly identical to the *in vivo* fluorescence imaging results (Fig. 4D).

Since a large percentage of melanoma metastases express melanin, we used the mouse B16F10 tumor xenograft model with endogenous expression of MC1R to determine the feasibility of using the NIRF probes for detection of melanotic lesions by fluorescence imaging. Fluorescence from the MC1RL-800 probe was not detectable at the 3 nmol/kg dosage using the Optix MX3 imaging system, but was detected using the FMT 2500 tomographic imaging instrument (Figure 4C). The probe concentration within the B16F10 tumors was determined to be 2120 ± 710 pMol. Hence, detection of fluorescence is possible in melanotic tumors but may be diminished as fluorescence was detected in the amelanotic A375 tumors with lower expression of MC1R using the same low dosage of probe and the Optix MX3 instrument. However, the use of higher dosages of probe or instrumental optimization could improve detection. Furthermore, detection of NIRF probes by a different imaging modality, such as multispectral optoacoustic tomography may have superior detection compared to fluorescence imaging.[46]

CONCLUSION

The MC1R specific fluorescent imaging probe with high affinity for the MC1R was successfully synthesized and characterized, and binding and uptake studies were performed. We have demonstrated that the probe can differentiate high- from low-MC1R expressing tumors *in vivo*. Therefore, MC1RL-800 is a promising molecular imaging probe for detection of MC1R-positive melanoma tumors and metastases in patients.

Targeted near-infrared fluorescence can be used for real-time intraoperative image-guidance with high resolution and sensitivity.[8] Therefore, our probe could be used to evaluate surgical margins of melanoma lesions and to detect regional lymph node metastasis in real-time during surgery. This capability could improve the rate of complete surgical resection of melanoma metastasis to a number of organ sites in melanoma patients whose tumors over-express MC1R, thereby decreasing the amount of tumor left behind and increasing tumor-free survival. Detection and removal of only lymph nodes that contain metastases would decrease morbidities associated with the non-specific removal of regional lymph nodes that do not have metastases during standard SLNB. Detection of fluorescence was possibly decreased in melanotic lesions relative to amelanotic lesions. Hence, the use of fluorescence for detection of melanoma may require optimization of the dosages administered and fluorescence instrumentation used, or use of a more sensitive modality, such as multispectral optoacoustic tomography may be required. In the future, the targeting ligand could be used to develop targeted radio-labeled PET or SPECT probes for the specific detection of melanoma metastases in the clinic, or as a MC1R targeted delivery vehicle for therapeutic agents.

Supplementary Material

Refer to Web version on PubMed Central for supplementary material.

Acknowledgments

The authors wish to acknowledge the Analytic Microscopy and Small Animal Modeling and Imaging Shared Resources at the H. Lee Moffitt Cancer Center & Research Institute, and the Comparative Biomedicine Department at the University of South Florida for their technical support. We also thank Michael Olive and LI-COR Biosciences for providing IRDye800CW. This work was supported by NIH/NCI R01CA097360, Morse PI.

Abbreviations

MC1R Melanocortin 1 receptor

References

(1). Siegel R, Naishadham D, Jemal A. Cancer statistics, 2012. CA Cancer J Clin. 2012; 62:10–29. [PubMed: 22237781]

(2). Thompson JF, Uren RF. Lymphatic mapping in management of patients with primary cutaneous melanoma. Lancet Oncol. 2005; 6:877–85. [PubMed: 16257796]

(3). Balch CM, Soong SJ, Gershenwald JE, Thompson JF, Reintgen DS, Cascinelli N, Urist M, McMasters KM, Ross MI, Kirkwood JM, Atkins MB, Thompson JA, Coit DG, Byrd D, Desmond R, Zhang Y, Liu PY, Lyman GH, Morabito A. Prognostic factors analysis of 17,600 melanoma patients: validation of the American Joint Committee on Cancer melanoma staging system. J Clin Oncol. 2001; 19:3622–34. [PubMed: 11504744]

(4). Kalady MF, White RR, Johnson JL, Tyler DS, Seigler HF. Thin melanomas: predictive lethal characteristics from a 30-year clinical experience. Ann Surg. 2003; 238:528–35. discussion 535-7. [PubMed: 14530724]

(5). Caudle AS, Ross MI. Metastasectomy for stage IV melanoma: for whom and how much? Surg Oncol Clin N Am. 2011; 20:133–44. [PubMed: 21111963]

(6). Ott PA, Berman RS. Surgical approach to primary cutaneous melanoma. Surg Oncol Clin N Am. 2011; 20:39–56. [PubMed: 21111958]

(7). Nguyen QT, Olson ES, Aguilera TA, Jiang T, Scadeng M, Ellies LG, Tsien RY. Surgery with molecular fluorescence imaging using activatable cell-penetrating peptides decreases residual cancer and improves survival. Proc Natl Acad Sci U S A. 2010; 107:4317–22. [PubMed: 20160097]

(8). van Dam GM, Themelis G, Crane LM, Harlaar NJ, Pleijhuis RG, Kelder W, Sarantopoulos A, de Jong JS, Arts HJ, van der Zee AG, Bart J, Low PS, Ntziachristos V. Intraoperative tumor-specific fluorescence imaging in ovarian cancer by folate receptor-alpha targeting: first in-human results. Nat Med. 2011; 17:1315–9. [PubMed: 21926976]

(9). Frangioni JV. New technologies for human cancer imaging. J Clin Oncol. 2008; 26:4012–21. [PubMed: 18711192]

(10). Keereweer S, Kerrebijn JD, van Driel PB, Xie B, Kaijzel EL, Snoeks TJ, Que I, Hutteman M, van der Vorst JR, Mieog JS, Vahrmeijer AL, van de Velde CJ, Baatenburg de Jong RJ, Lowik CW. Optical image-guided surgery--where do we stand? Mol Imaging Biol. 2011; 13:199–207. [PubMed: 20617389]

(11). Balch CM. [Diagnosis and prognosis of malignant melanoma]. Dtsch Med Wochenschr. 1985; 110:1783–6. [PubMed: 2414087]

(12). Hinz T, Ahmadzadehfar H, Wierzbicki A, Hoeller T, Wenzel J, Biersack HJ, Bieber T, Schmid-Wendtner MH. Sentinel lymph node status as most important prognostic factor in patients with high-risk cutaneous melanomas (tumour thickness >4.00 mm): outcome analysis from a single institution. Eur J Nucl Med Mol Imaging. 2012

(13). Hettiaratchy SP, Kang N, O'Toole G, Allan R, Cook MG, Powell BW. Sentinel lymph node biopsy in malignant melanoma: a series of 100 consecutive patients. Br J Plast Surg. 2000; 53:559–62. [PubMed: 11000070]

(14). Cigna E, Gradilone A, Ribuffo D, Gazzaniga P, Fino P, Sorvillo V, Scuderi N. Morbidity of selective lymph node biopsy for melanoma: meta-analysis of complications. Tumori. 2012; 98:94–8. [PubMed: 22495708]

(15). Crane LM, Themelis G, Buddingh K, Harlaar NJ, Pleijhuis RG, Sarantopoulos A, van der Zee AG, Ntziachristos V, van Dam GM. Multispectral real-time fluorescence imaging for intraoperative detection of the sentinel lymph node in gynecologic oncology. J Vis Exp. 2010

(16). Wagner JD. A role for FDG-PET in the surgical management of stage IV melanoma. Ann Surg Oncol. 2004; 11:721–2. [PubMed: 15249339]

(17). Hsu M, Andl T, Li G, Meinkoth JL, Herlyn M. Cadherin repertoire determines partner-specific gap junctional communication during melanoma progression. J Cell Sci. 2000; 113(Pt 9):1535–42. [PubMed: 10751145]

(18). Wang R, Kobayashi R, Bishop JM. Cellular adherence elicits ligand-independent activation of the Met cell-surface receptor. Proc Natl Acad Sci U S A. 1996; 93:8425–30. [PubMed: 8710887]

(19). Yang P, Farkas DL, Kirkwood JM, Abernethy JL, Edington HD, Becker D. Macroscopic spectral imaging and gene expression analysis of the early stages of melanoma. Mol Med. 1999; 5:785–94. [PubMed: 10666478]

(20). Siegrist W, Solca F, Stutz S, Giuffre L, Carrel S, Girard J, Eberle AN. Characterization of receptors for alpha-melanocyte-stimulating hormone on human melanoma cells. Cancer Res. 1989; 49:6352–8. [PubMed: 2804981]

(21). Cai M, Varga EV, Stankova M, Mayorov A, Perry JW, Yamamura HI, Trivedi D, Hruby VJ. Cell signaling and trafficking of human melanocortin receptors in real time using two-photon fluorescence and confocal laser microscopy: differentiation of agonists and antagonists. Chem Biol Drug Des. 2006; 68:183–93. [PubMed: 17105482]

(22). Koikov LN, Ebetino FH, Solinsky MG, Cross-Doersen D, Knittel JJ. Sub-nanomolar hMC1R agonists by end-capping of the melanocortin tetrapeptide His-D-Phe-Arg-Trp-NH(2). Bioorg Med Chem Lett. 2003; 13:2647–50. [PubMed: 12873485]

(23). Mayorov AV, Han SY, Cai M, Hammer MR, Trivedi D, Hruby VJ. Effects of macrocycle size and rigidity on melanocortin receptor-1 and - 5 selectivity in cyclic lactam alpha-melanocyte-stimulating hormone analogs. Chem Biol Drug Des. 2006; 67:329–35. [PubMed: 16784457]

(24). Geschwind, Huseby RA, Nishioka R. The effect of melanocyte-stimulating hormone on coat color in the mouse. Recent Prog Horm Res. 1972; 28:91–130. [PubMed: 4631622]

(25). Hunt G, Kyne S, Wakamatsu K, Ito S, Thody AJ. Nle4DPhe7 alpha-melanocyte-stimulating hormone increases the eumelanin:phaeomelanin ratio in cultured human melanocytes. J Invest Dermatol. 1995; 104:83–5. [PubMed: 7798647]

(26). Tamate HB, Takeuchi T. Action of the e locus of mice in the response of phaeomelanic hair follicles to alpha-melanocyte-stimulating hormone in vitro. Science. 1984; 224:1241–2. [PubMed: 6328651]

(27). Gong R. The renaissance of corticotropin therapy in proteinuric nephropathies. Nat Rev Nephrol. 2012; 8:122–8. [PubMed: 22143333]

(28). Chen J, Giblin MF, Wang N, Jurisson SS, Quinn TP. In vivo evaluation of 99mTc/188Re-labeled linear alpha-melanocyte stimulating hormone analogs for specific melanoma targeting. Nucl Med Biol. 1999; 26:687–93. [PubMed: 10587108]

(29). Cai M, Mayorov AV, Cabello C, Stankova M, Trivedi D, Hruby VJ. Novel 3D pharmacophore of alpha-MSH/gamma-MSH hybrids leads to selective human MC1R and MC3R analogues. J Med Chem. 2005; 48:1839–48. [PubMed: 15771429]

(30). Handl HL, Vagner J, Yamamura HI, Hruby VJ, Gillies RJ. Lanthanide-based time-resolved fluorescence of in cyto ligand-receptor interactions. Anal Biochem. 2004; 330:242–50. [PubMed: 15203329]

(31). Yang Y, Hruby VJ, Chen M, Crasto C, Cai M, Harmon CM. Novel binding motif of ACTH analogues at the melanocortin receptors. Biochemistry. 2009; 48:9775–84. [PubMed: 19743876]

(32). Barkey NM, Tafreshi NK, Josan JS, De Silva CR, Sill KN, Hruby VJ, Gillies RJ, Morse DL, Vagner J. Development of melanoma-targeted polymer micelles by conjugation of a melanocortin 1 receptor (MC1R) specific ligand. J Med Chem. 2011; 54:8078–84. [PubMed: 22011200]

(33). Morse DL, Carroll D, Weberg L, Borgstrom MC, Ranger-Moore J, Gillies RJ. Determining suitable internal standards for mRNA quantification of increasing cancer progression in human

breast cells by real-time reverse transcriptase polymerase chain reaction. Anal Biochem. 2005; 342:69–77. [PubMed: 15958182]

(34). Xu L, Vagner J, Alleti R, Rao V, Jagadish B, Morse DL, Hruby VJ, Gillies RJ, Mash EA. Synthesis and characterization of a Eu-DTPA-PEGO-MSH(4) derivative for evaluation of binding of multivalent molecules to melanocortin receptors. Bioorg Med Chem Lett. 2010; 20:2489–92. [PubMed: 20304640]

(35). Cheng Z, Xiong Z, Subbarayan M, Chen X, Gambhir SS. 64Cu-labeled alpha-melanocyte-stimulating hormone analog for microPET imaging of melanocortin 1 receptor expression. Bioconjug Chem. 2007; 18:765–72. [PubMed: 17348700]

(36). Baumann JB, Bagutti C, Siegrist W, Christen E, Zumsteg U, Eberle AN. MSH receptors and the response of human A375 melanoma cells to interleukin-1 beta. J Recept Signal Transduct Res. 1997; 17:199–210. [PubMed: 9029491]

(37). JAI Press; Greenwich, Conn: 1997. p. v

(38). Bullok KE, Gammon ST, Violini S, Prantner AM, Villalobos VM, Sharma V, Piwnica-Worms D. Permeation peptide conjugates for in vivo molecular imaging applications. Mol Imaging. 2006; 5:1–15. [PubMed: 16779965]

(39). Knight LC. Non-oncologic applications of radiolabeled peptides in nuclear medicine. Q J Nucl Med. 2003; 47:279–91. [PubMed: 14973420]

(40). Okarvi SM. Recent progress in fluorine-18 labelled peptide radiopharmaceuticals. Eur J Nucl Med. 2001; 28:929–38. [PubMed: 11504093]

(41). Okarvi SM. Peptide-based radiopharmaceuticals: future tools for diagnostic imaging of cancers and other diseases. Med Res Rev. 2004; 24:357–97. [PubMed: 14994368]

(42). Koikov LN, Ebetino FH, Solinsky MG, Cross-Doersen D, Knittel JJ. Analogs of sub-nanomolar hMC1R agonist LK-184 [Ph(CH2)3CO-His-D-Phe-Arg-Trp-NH2]. An additional binding site within the human melanocortin receptor 1? Bioorg Med Chem Lett. 2004; 14:3997–4000. [PubMed: 15225714]

(43). Di L, Kerns EH. Profiling drug-like properties in discovery research. Curr Opin Chem Biol. 2003; 7:402–8. [PubMed: 12826129]

(44). Cheng Z, Zhang L, Graves E, Xiong Z, Dandekar M, Chen X, Gambhir SS. Small-animal PET of melanocortin 1 receptor expression using a 18F-labeled alpha-melanocyte-stimulating hormone analog. J Nucl Med. 2007; 48:987–94. [PubMed: 17504880]

(45). Stein WD, Litman T, Fojo T, Bates SE. A Serial Analysis of Gene Expression (SAGE) database analysis of chemosensitivity: comparing solid tumors with cell lines and comparing solid tumors from different tissue origins. Cancer Res. 2004; 64:2805–16. [PubMed: 15087397]

(46). Razansky D, Deliolanis NC, Vinegoni C, Ntziachristos V. Deep tissue optical and optoacoustic molecular imaging technologies for pre-clinical research and drug discovery. Curr Pharm Biotechnol. 2012; 13:504–22. [PubMed: 22216767]

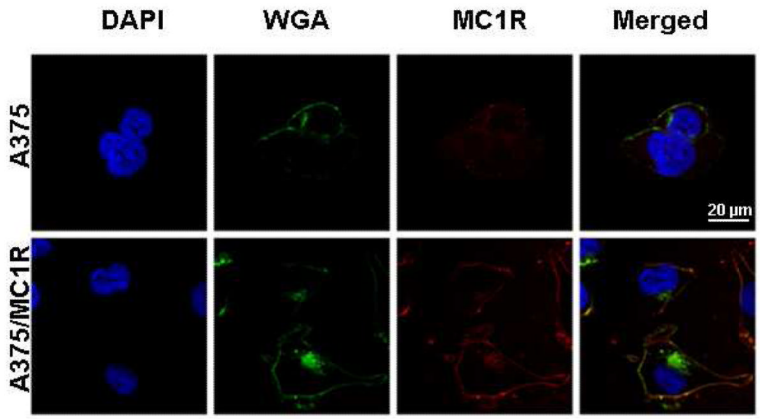

Figure 1.

ICC of MC1R expression on the surface of A375 parental and engineered cells. Confocal micrographs of cells incubated with the nuclear marker DAPI (blue), the plasma- and plasma-membrane marker, WGA (green) and MC1R antibody-Alexa 555 (red). To inhibit cellular uptake, cells were incubated with antibodies and dyes at 4°C for 10 min. The merged image shows co-localization of MC1R (red) with membrane marker (green) indicating accumulation of the receptor on the cell-surface (yellow).

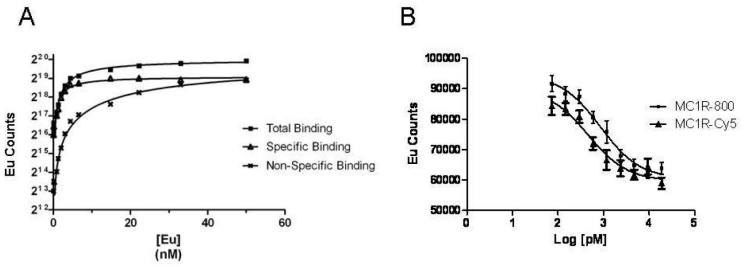

Figure 2.

(A) Representative saturation binding assays for A375/hMC1R cells. (B) A representative competition binding plot of MC1RL-800 imaging probe to A375/hMC1R cells.

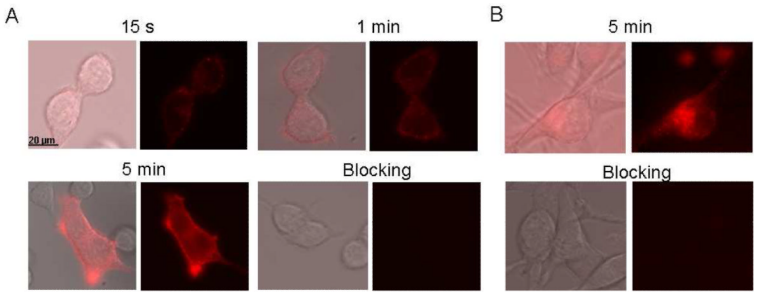

Figure 3.

In vitro uptake studies of the MC1RL-Cy5 targeted imaging probe. (A) Fluorescence microscopy images at 15 s, 1 min and 5 min following addition of probe to an incubation chamber containing A375/MC1R cells grown on a coverslip. Probe binding is observed by 15 s and internalization by 5 mins. (B) Fluorescence microscopy images of probe uptake by B16 cells at the 5 min time-point showing internalization of probe into the cells. For both panels A and B, images are included for blocking studies at the 5 min time-point, where cells were pre-incubated with the unlabeled melanocortin-receptor ligand, NDP-α-MSH, prior to addition of probe. Pre-incubation with unlabeled ligand completely blocked binding and uptake of probe. For both panels A and B, the image on the left of each pair shows the overlay of the fluorescence image on the visible light (differential interference contrast) image of the corresponding cells and the left panel shows only the fluorescence.

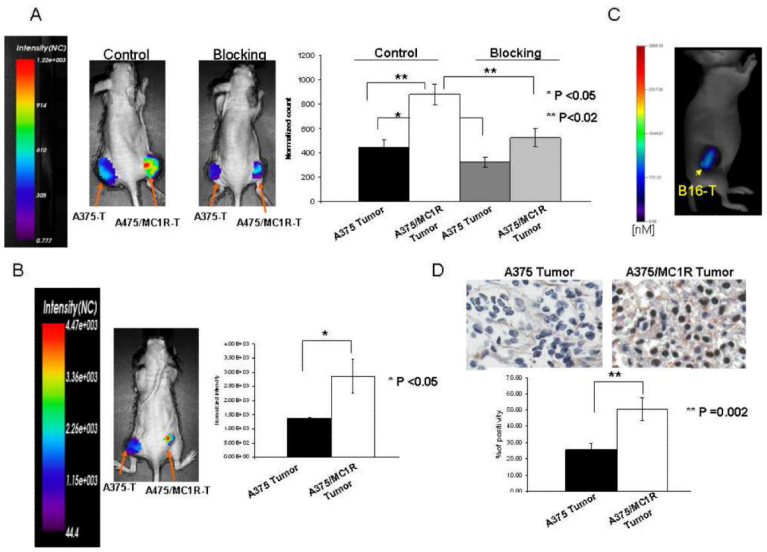

Figure 4.

In vivo targeting of MC1R specific probe. (A) Representative images of normalized fluorescence intensity maps overlayed on mice bearing xenograft tumors. A375 cells that constitutively express low levels of MC1R were used to form the low-expressing tumor (left flank) and A375/MC1R cells were used to form the high expressing tumor (right flank). The control image (left mouse) shows lower fluorescence signal in the left flank tumor relative to the right flank tumor 4 hours after intravenous injection of 3 nmol/kg of the MC1RL-800 probe. A blocking experiment (right mouse) was performed by co-injection of 0.25 μg unlabeled NDP-α-MSH and 3 nmol/kg of the MC1RL-800 probe to demonstrate specific binding. Inset on the far right graphs normalized fluorescence counts that significantly vary among low and high expressing tumors, and among tumors in control experiments compared to blocking experiments. (B) Representative image at 4 hours after injection of 3 nmol/kg of the MC1RL-Cy5 probe. Graph shows relative quantification of fluorescence in low and high expressing tumors. For panels A & B, images were acquired using the Optix-MX3 imaging system (Advanced Research Technologies, Inc.), graphed data represent the mean ± s.d., and NC = Normalized Counts. (C) Representative tomographic image of a mouse bearing a B16F10 xenograft tumor at 4 hours after injection of 3 nmol/kg of the MC1RL-800 imaging probe using the FMT 2500 LX quantitative fluorescence tomography *in vivo* imaging system (PerkinElmer). (D) MC1R IHC staining of A375 and A375/MC1R xenograft tumors. The bar graph shows the quantification of MC1R staining. Data represent mean ± s.d..

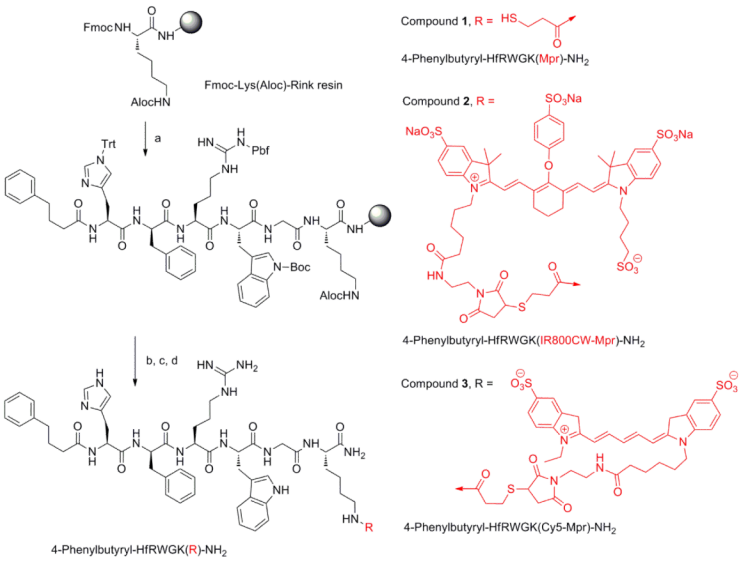

SCHEME 1. Synthetic route for Cy5 and IRDye800CW ligands

a. Fmoc/*t*Bu synthesis continued as follows: i) Fmoc-aa-OH (3eq), HOBt (3eq), DIEA (6eq), and HBTU (3eq) in DMF for amino acid couplings; ii) Piperidine/DMF (1:4) for Fmoc deprotection; b. Aloc deprotection: i) Pd(0)TPP_4 (0.2eq), dimethylbarbituric acid (5.0 eq) in DCM (0.5 M) for 30 min' ii) Trt-OH (3eq), DIEA (6eq), and HBTU (3eq) in DMF; c. TFA-scavengers cocktail (91% trifluoroacetic acid, 3% water, 3% triisopropylsilane, and 1,2-ethylenedithiol (3%) for 4 hrs; d. IRDye800CW maleimide or Cy5 maleimide (1eq) in DMF.